Interaction of the Isolated Transmembrane Domain of Diphtheria Toxin with Membranes†

Hangjun Zhan,‡ Kyoung Joon Oh,§ Yeon-Kyun Shin,§ Wayne L. Hubbell,§ and R. John Collier*,‡

Department of Microbiology and Molecular Genetics and Shipley Institute of Medicine, Harvard Medical School, 200 Longwood Avenue, Boston, Massachusetts 02115, and Jules Stein Eye Institute and Department of Chemistry and Biochemistry, University of California, Los Angeles, California 90024

Received December 19, 1994; Revised Manuscript Received February 3, 1995⊗

ABSTRACT: Insertion of diphtheria toxin's T (transmembrane) domain into the endosomal membrane under acidic conditions is known to promote translocation of its catalytic domain across the membrane and into the cytosol. The T domain, a cysteine-free bundle of α-helices, was expressed as a discrete protein in *Escherichia coli* and purified. The isolated domain was stable and largely monomeric at pH 8.0. Like the holotoxin it bound the hydrophobic fluorophore, 2-*p*-toluidinylnaphthalene 6-sulfonate, upon acidification, but the transition pH was higher than with the holotoxin (pH 5.6 vs 5.1) and broader, reflecting the absence of interdomain interactions. The domain also permeabilized large unilamellar vesicles under acidic conditions, as demonstrated by release of entrapped solutes. Mutant forms of T domain, each with a single residue replaced by cysteine, were derivatized with a thiol-reactive nitroxide-containing spin label and analyzed by electron paramagnetic resonance (EPR). EPR spectra and solvent accessibilities of the labels at pH 8.0 were consistent with the environments predicted from the toxin's crystallographic structure. Acidification in the presence of large unilamellar vesicles caused a nitroxide label at position 332 on helix TH8 to move from a buried site in the water soluble state to a lipid-exposed surface site at a depth of ~15 Å within the bilayer. This is consistent with the concept that the TH8−TH9 helix pair inserts into the bilayer. Changes in the nitroxide at residue 351 suggest that this side chain, located in the loop linking helices TH8 and TH9, moves to a buried site within the tertiary fold of a reorganized monomer or within an oligomeric structure formed in the membrane. These findings validate the isolated T domain as an object of investigation and demonstrate the potential of site-directed spin labeling for elucidating the structure of diphtheria toxin within membranes.

Many toxic proteins are known to be extraordinary enzymes, having the ability to deliver their catalytic moieties to the cytosolic compartment of mammalian cells. Although toxin entry into cells has been investigated in many systems, the process by which the catalytic moiety is translocated across membranes remains poorly described in general and is not understood in detail for any toxin.

Diphtheria toxin (DT)[1] has been extensively studied as a model of protein toxins (Collier, 1990), and considerable effort has been devoted to understanding its mechanism of membrane translocation (Olsnes *et al.,* 1991; London, 1992). The toxin, a single 535-residue polypeptide, is proteolytically cleaved into two fragments before or during its action on mammalian cells. The resulting N-terminal fragment (DTA; 193 residues) is the catalytic moiety, whereas the C-terminal 37 kDa fragment (DTB; 342 residues) binds the toxin to receptors and mediates translocation of DTA into the cytoplasm. Once in the cytoplasm, DTA catalyzes the ADP-ribosylation of elongation factor-2, which inhibits protein synthesis and causes cell death.

After binding to its receptor (Naglich *et al.,* 1992), DT undergoes receptor-mediated endocytosis and is transported to the endosomal compartment. There, the acidic pH triggers conformational changes in the toxin, inducing it to insert into the endosomal membrane and to become an integral membrane protein. This step is crucial for translocation of DTA across the endosomal membrane and thus for toxicity (O'Keefe *et al.,* 1992; Silverman *et al.,* 1994). Receptor-bound toxin is capable of forming channels in the plasma membrane when the extracellular medium is acidified, and similar channels are formed by the toxin alone in artificial lipid bilayers. The membrane insertion and channel formation functions are localized to the N-terminal region of DTB.

The crystallographic structure of DT reveals a Y-shaped molecule of three domains: the catalytic domain (C), the translocation domain (T), and the receptor binding domain (R) (Choe *et al.,* 1992; Bennett *et al.,* 1994; Bennett & Eisenberg, 1994). DTA corresponds to domain C and DTB to domains T and R. The T domain, which contains the membrane-insertion region of DTB, consists of nine α-helices arranged in three layers (Figure 1). The innermost layer is a buried hydrophobic pair of helices (TH8 and TH9)

†This work was supported by NIH Grants AI-22021 (R.J.C.), AI-22848 (R.J.C.), and EY-05216 (W.L.H.) and by the Jules Stein Professor Endowment (W.L.H.).

* To whom correspondence should be addressed.

‡ Harvard Medical School.

§ University of California, Los Angeles.

⊗ Abstract published in *Advance ACS Abstracts,* March 15, 1995.

[1] Abbreviations: ANTS, 8-aminonaphthalene-1,3,6-trisulfonic acid; DOPG, 1, 2-dioleoyl-*sn*-glycero-3-phosphatidylglycerol; DPX, *p*-xylene-bispyridinium bromide; DT, diphtheria toxin; DTT, dithiothreitol; EDDA, ethylenediaminediacetic acid; EDTA, ethylenediaminetetraacetic acid; EPR, electron paramagnetic resonance; LUV, large unilamellar vesicles; NiAA, nickel(II)acetylacetone; NiEDDA, nickel(II)ethylenediamine diacetate; PC, phosphatidylcholine; SDS−PAGE, sodium dodecyl sulfate−polyacrylamide gel electrophoresis; SUV, small unilamellar vesicles; TNS, 2-*p*-toluidinylnaphthalene 6-sulfonate; Tris, tris(hydroxymethyl)aminomethane.

0006-2960/95/0434-4856$09.00/0

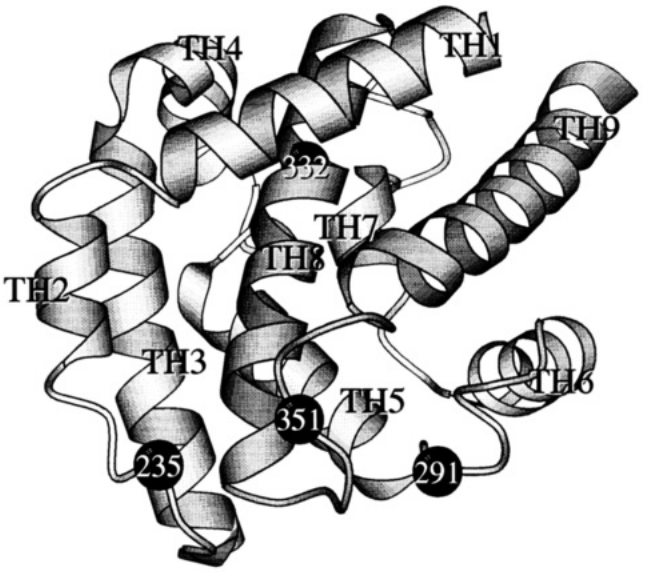

FIGURE 1: Structure of the diphtheria toxin T domain (residues 202−378). The locations of four residues selected for mutation to cysteine and attachment of spin probes are indicated. This Molscript representation (Kraulis, 1991) was generated using the coordinates of diphtheria toxin provided by M. J. Bennett and D. Eisenberg (Bennett *et al.,* 1994).

connected by a loop (TL5) containing two acidic residues (E349 and D352). The intermediate layer consists of helices TH5−TH7, which form another hydrophobic and kinked hairpin wrapped around TH8 and TH9. The outermost layer (helices TH1−TH4) is highly charged and unlikely to insert into a bilayer at any pH.

To dissect the structure and function of the T domain, we have expressed it as a discrete protein and investigated its interaction with lipid vesicles. Characterization of conformational changes occurring during membrane insertion requires that we understand its structure both in the soluble and membrane-bound states. Determination of the structure of membrane-bound proteins at atomic resolution has proven to be difficult, and no general approach has yet emerged. However, the method of site-directed spin-labeling offers an attractive strategy for obtaining a highly detailed portrait of topography as well as for determining secondary and tertiary structure in membrane proteins (Altenbach *et al.,* 1990; Shin *et al.,* 1993; Altenbach *et al.,* 1994; Hubbell & Altenbach, 1994). In this study, we have taken the first steps to apply site-directed spin-labeling to the elucidation of the detailed intramembrane structure of DT.

MATERIALS AND METHODS

Design and Construction of the T-Domain Expression Vector. Expression vector pET-15b (Novagen) was used for expression of the T domain. Due to the lack of appropriate restriction sites for direct T domain DNA cloning, an *Nde*1 site at the 5′ end of the T-domain and the *Eco*R1 at the 3′ end of the domain were introduced by the polymerase chain reaction (PCR) (Figure 2). Primer I containing a *Nde*1 site in the overhang sequence was 5′-GGC AGC **CAT ATG** ATA AAT CTT GAT TGG GAT GTC. Primer II (the reverse primer) encoded a stop codon followed by an *Eco*RI site: 5′-TAT GC**G AAT *TC*A *TCA*** GGG ACG ATT ATA CGA ATT ATG. The annealing (complementary) sequences of the primers are underlined, double stop codons are italicized, and restriction sites are in boldface. The template

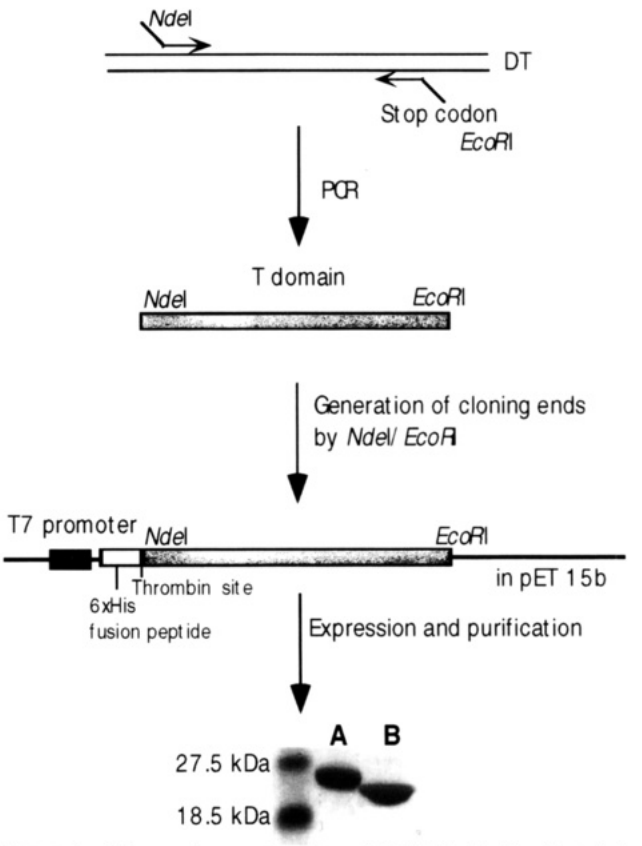

FIGURE 2: Scheme for construction of pET-15b-T. See Materials and Methods for details. (Last panel) Coomassie-stained SDS−polyacrylamide gel showing the T domain with (A) and without (B) the hexa-histidine tag.

for PCR was pDO1 (O'Keefe *et al.,* 1992). DNA fragments from PCR were digested with restriction endonucleases *Nde*I and *Eco*RI, and the fragments were gel purified and cloned into expression vector pET-15b (Novagen), generating pET-15b-T. The entire T-domain DNA sequence and its junctions to the vector were confirmed by double-stranded DNA sequencing after alkaline denaturation. pET-15b-T was used for T-domain overexpression and purification.

Expression and Purification of T Domain Protein. Expression and purification procedures were as described in the pET system manual from Novagen. Plasmid pET-15b-T was introduced into *Escherichia coli* BL21(DE3) (Studier & Moffatt, 1986) by electroporation, and the T domain was expressed cytoplasmically. Cultures of $A_{600} = 0.8-1.0$ were induced by adding isopropyl β-D-thiogalactopyranoside (IPTG) to a final concentration of 1 mM, and after 2 h at 37 °C or 4 h at 30 °C, cells were harvested and sonicated on ice, using a Sonifier Cell Disruptor 350 (Branson Sonic Power Co.) with the power control at 5 and the duty cycle at 50%. The cell debris was pelleted by centrifugating at 12000*g* for 30 min at 4 °C. Optimal yields of T domain in the cytoplasmic fraction of *E. coli* were obtained when induction was performed at 37 °C for no more than 2 h or at 30 °C for 4 h. Protein was purified from the soluble fraction, and inclusion bodies were discarded. The supernatants were collected and loaded directly onto a 2−3 mL nickel chelate affinity column. After washing, the proteins were eluted with 1 M imidazole. The eluents were dialyzed against 20 mM Tris-HCl buffer, pH 8.0, for 16 h at 4 °C with three changes of buffer. The protein samples were concentrated using a Centriprep 10 (MW cut-off, 10 kDa)

(Amicon). The samples were further concentrated by using a Centricon 10 (Amicon) if necessary. The N-terminal hexahistidine tail was removed proteolytically with thrombin. The protein purified in this manner has four additional residues at the N-terminus: Gly-Ser-His-Met. To avoid confusion, however, the numbering of residues is that of native DT (Greenfield *et al.*, 1983). Further purification was accomplished by anion-exchange FPLC chromatography (Mono Q, Pharmacia, or MemSep, Millipore), in 20 mM Tris-HCl, pH 8.0, with a NaCl gradient from 0 to 1 M. T domain was eluted at ~150 mM NaCl as a single peak. The protein samples were stored in Tris-HCl buffer (20 mM, pH 8.0).

All PCRs were performed with Vent DNA Polymerase (exo^+; New England Biolabs). The western immunoblots were performed with anti-DT antiserum (Cannaught) as the primary antibody and alkaline phosphatase-conjugated rabbit anti-horse IgG (Sigma) as the secondary antibody. Blots were developed with 5-bromo-4-chloro-3-indolyl phosphate as the chromagenic substrate. Protein concentrations were determined by the Bradford method with Protein Assay Reagent (Pierce) with bovine serum albumin as control.

Analysis of T Domain by HPLC. The T domain was analyzed by gel filtration HPLC using a Superdex 75 HR 10/30 column (Pharmacia). The protein sample was diluted in 50 mM Tris-HCl buffer (0.1 M KCl, pH 8.0) or in 100 mM sodium acetate buffer (0.15 M KCl, pH 4.6) to a final volume of 50 μL prior to injection. Twenty microliters of the diluted protein solution was injected onto the column. Protein was eluted with the corresponding buffer at a flow rate of 1.0 mL/min at room temperature. A mixture of bovine gamma globulin, bovine serum albumin, chicken ovalbumin, equine myoglobin, cytochrome *c*, and vitamin B-12 was used as molecular weight standards.

Preparation of SUVs with Entrapped Fluorophores. A lipid mixture (20 mg) composed of 20% DOPG and 80% PC (w/w) in $CHCl_3$ was dried uniformly onto the sides of a 25 mL pear-shaped flask under a stream of nitrogen and further dried under high vacuum for 3 h. To prepare the SUV stock, the lipids were resuspended in 2 mL of 12.5 mM ANTS, 45 mM DPX, 45 mM NaCl, 10 mM Tris-HCl, and 0.1 mM EDTA, pH 7.5, by vortexing and then sonicated on ice in a Branson Model 350 Sonifier to near optical clarity. Care was taken to avoid heating during the sonication. After sonication, unencapsulated ANTS and DPX were separated from liposomes by gel filtration on a Sephadex G-50 column (1 × 25cm) equilibrated with 10 mM Tris-HCl, 0.1 mM EDTA, and 140 mM NaCl, pH 7.5. The phospholipid content of the liposomes was determined by inorganic phosphate analysis (McClare, 1971).

Monitoring Insertion of T Domain by Fluorescence. T domain insertion into vesicle membranes was measured by an ANTS/DPX fluorescence leakage assay as described (Mel & Stroud, 1993). To determine dose−response curves for the T domain, different amounts of T domain were incubated with a solution of liposomes (50 μM final phospholipid concentration in 10 mM Tris-HCl, 140 mM NaCl, and 0.1 mM EDTA, pH 7.5) with constant stirring in a quartz cuvette at 25 °C. The mixture was monitored for 100 s to determine the baseline fluorescence leakage, at which time a predetermined amount of 0.5 M sodium acetate (pH 4.3) was added to adjust the final pH to 5.0. The final volume of each reaction mixture was 2 mL. Fluorophore release was recorded for 300 s; then 5 μL of 5% Triton X-100 was added to each 2 mL sample to lyse the liposomes, and the mixture was monitored for an additional 100 s. The T domain caused no change at neutral pH, a property also shared by whole toxin. All the fluorescence data were recorded with an excitation wavelength of 360 nm and emission wavelength of 550 nm.

Fluorimetric Detection of Conformational Changes in T Domain. The detailed protocol was as previously described (Koehler & Collier, 1991). T domain at a final concentration of 330 nM was incubated with 150 μM TNS for 20−30 min at room temperature in 100 mM buffer (Tris-HCl, for pH 8.0 and 7.0; Mes for pH 6.5 and 6.0; sodium acetate for pH 5.5, 5.25, 5.0, 4.75, and 4.5) containing 150 mM NaCl and 1 mM EDTA. Fluorescence emission was recorded with excitation wavelength of 366 nm and emission wavelength of 440 nm. All the fluorescence measurements were made with constant stirring at 25 °C using an Aminco SLM spectrofluorometer 500 equipped with a thermostated cell.

Site-Directed Cys Mutagenesis of the T Domain. Oligonucleotides were synthesized on an Applied Biosystems Model 381A DNA synthesizer and purified as previously described (Hovde *et al.*, 1988). Site-directed cysteine mutagenesis was performed with the Oligonucleotide Directed *in vitro* Mutagenesis System, Version 2.1 (Amersham), according to manufacturer's instructions. Phage M13mp18::DT vector containing the entire diphtheria toxin gene sequence (with the E148S substitution to ablate enzyme activity) was constructed by inserting the *Bam*HI−*Eco*RI fragment containing the DT sequence from pDOl (O'Keefe *et al.*, 1992) into M13mp18. The single-stranded M13mp18::DT was used as the template for mutagenesis. Mutations were screened and verified by DNA sequencing with the Sequenase kit (United States Biochemicals). All other DNA manipulations were performed as described by Ausubel *et al.*, (1987). Mutant proteins were purified as described above for the wild-type T domain. The presence of the engineered cysteine in each mutant protein was verified by removing the reducing agent and labeling with fluorescein maleimide. The labeled proteins were resolved by SDS−polyacrylamide gel electrophoresis, and their fluorescence was detected by irradiation of the gel with an ultraviolet transilluminator.

Spin Labeling of T Domain Cysteine Mutants. T domain (100−200 μg; 0.5−1.5 mg/mL) in 20 mM Tris, pH 8.0, and 2 mM DTT was concentrated to a final volume of about 0.1 mL by centrifugation using a Microcon 10 (Amicon, Beverly, MA). Concentrated protein was added to a 1.5 mL volume of 2 mM (1-oxyl-2,2,5,5-tetramethylpyrroline-3-methyl)-methanethiosulfonate spin label in 20 mM Tris, pH 8.0, at room temperature, and the mixture shaken gently overnight. Unreacted spin label was removed by dialysis at 4 °C against 20 mM Tris buffer, pH 8.0. After dialysis, the protein was concentrated using a Microsep centrifugal concentrator (Filtron Technology corporation, Northborough, MA). The concentration of the spin-labeled protein was determined by the Bradford assay using BSA as a standard. Proteins were stored at 4 °C and never frozen. EPR spectra were recorded at room temperature on a Varian E-9 EPR spectrometer equipped with a loop gap resonator (Hubbell *et al.*, 1987). Power saturation experiments on spin-labeled T domain in the presence of various concentrations of NiEDDA or O_2 were carried out in TPX capillaries (Altenbach *et al.*, 1989). Saturation curves were analyzed in terms of the accessibility

parameter, Π, as previously described (Farahbakhsh *et al.*, 1992; Hubbell & Altenbach, 1994).

Preparation of LUVs. LUV suspensions containing 17 mol % 1-palmitoyl-2-oleoyl-*sn*-glycero-3-phospho-*rac*-(1-glycerol) (POPG) in 1-palmitoyl-2-oleoyl-*sn*-glycero-3-phosphocholine (POPC) were prepared by reverse-phase evaporation according to Szoka and Papahadjopoulos (1978), followed by extrusion. Briefly, 20 mg of POPG and 100 mg of POPC (both from Avanti, Birmingham, AL) were dissolved in 7.2 mL of diethyl ether, sodium acetate buffer (2.4 mL, 100 mM, pH 4.3) was added, and the mixture was sonicated on a bath-type sonicator for 1−2 min. Vesicles were formed by evaporating the ether under reduced pressure, and LUVs were prepared by extruding the resulting multilamellar vesicles 10−15 times through two sheets of polycarbonate membrane with a pore size of 100 nm (Avestin). The phospholipid concentration of the vesicles was determined using the Böttcher-modified Bartlett assay (Böttcher *et al.*, 1961). The phospholipid concentration ranged from 50 to 60 mM depending on the vesicle preparations.

Preparation of Membrane-Bound T Domain. The pH of an LUV suspension prepared as described above was raised to pH 6.8 using 1 N NaOH just prior to protein addition. Four microliters of an approximately 10 mg/mL stock solution of T domain was then added. To induce binding, 20 μL of 100 mM sodium acetate, pH 4.3, was added to the protein/vesicle solution (final pH = 4.6). The molar ratio of T domain to phospholipid was approximately 1:500. The resulting turbid solution was centrifuged at 15000*g* for 15 min at 4 °C. EPR measurements showed that most of the spin-labeled protein was in the vesicle pellet. To introduce NiEDDA, the desired volume of a 50 mM NiEDDA solution in methanol was transferred to an Eppendorf tube and the solvent evaporated under reduced pressure. The vesicle preparation described above was added to the solid NiEDDA and mixed throughly.

RESULTS AND DISCUSSION

A DNA segment encoding the T domain (residues 202−378 of DT) was incorporated into expression vector pET-15b, which fused a hexahistidine-containing peptide to the domain's N-terminus and placed expression under control of the T7 promoter. The T domain *per se* contains no cysteines, and the choice of Ile-202 as the N-terminal residue eliminated the only nearby cysteine, Cys-201. Extracts from *E. coli* expressing the fusion protein were centrifuged to remove any toxin-related protein within inclusion bodies, and the protein was purified from the soluble fraction. Selective adsorption to a Ni^{2+} chelate column and elution with imidazole-containing buffer yielded a relatively pure product, which was digested with thrombin to remove the affinity tag (Figure 2), and the products were fractionated by anion exchange chromatography. The purified domain (purity >95%, as determined by scanning densitometry of SDS−polyacrylamide gels) was dialyzed against 20 mM Tris-HCl buffer, pH 8.0, and stored at 4 °C. Routinely, ~2.5 mg of pure protein was obtained from a 1 L culture. The protein (calculated M_r 19 181; calculated pI 4.76) was water-soluble and stable for weeks at 4 °C. It reacted with antiserum against DT, as determined by Western blotting.

Conformational changes occurring in the T domain under acidic conditions were compared with those in the holotoxin

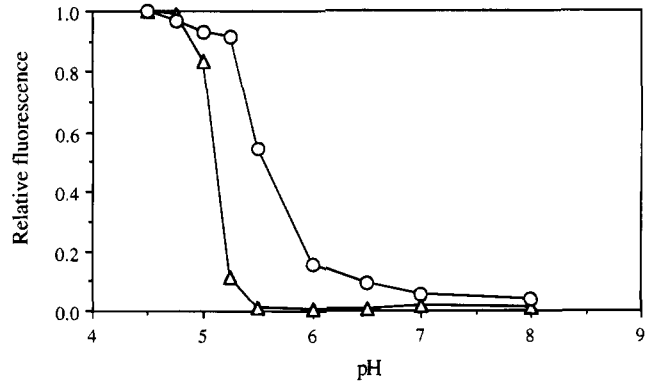

FIGURE 3: pH-dependent association of TNS with T domain or DT. Each protein was diluted to 330 nM in 150 μM TNS at pH 8.0, 7.0, 6.5, 6.0, 5.5, 5.25, 5.0, 4.75, or 4.5 and incubated for 20 min at room temperature, and the fluorescence was determined at 25 °C (excitation wavelength 366 nm; emission wavelength 440 nm). T domain (○); whole DT (×c6△). The DT was largely (91%) free from the endogenous dinucleotide, ApUp, as determined from absorbance values at 260 and 280 nm (O'Keefe, 1992).

by fluorescence measurements in the presence of TNS, a fluorophore that has been used to detect exposure of hydrophobic sites on proteins (Figure 3). Samples of DT or T domain were incubated with 150 μM TNS for 20 min at various pH values (at room temperature) before fluorescence readings were taken. Consistent with earlier results (Sandvig & Olsnes, 1991; Dumont & Richards, 1988; Silverman *et al.*, 1994), the holotoxin gave a sharp titration curve, with little TNS fluorescence above pH 5.5, a half-maximum at pH 5.1, and maximum at pH ~4.75. With isolated T domain, the transition was broader and occurred at a higher pH (half-maximum at pH 5.6). Decreasing the TNS concentration to 50 or 5 μM did not alter the midpoints of the titration curves, and the readings did not change with time (over 1 h), implying that the fluorescence reflected equilibrium binding to a conformationally altered form of the protein.

The fact that the transition occurred at a lower pH with the holotoxin than with the T domain implies that there are constraints outside the T domain that influence pH-dependent conformational changes within the holotoxin. Bennett and co-workers (Bennett & Eisenberger, 1994; Bennett et al., 1994) have described three salt bridges between the C and R domains and five between T and C, which may stabilize the holotoxin relative to the T domain. The sharper titration curve of the holotoxin presumably reflects cooperativity in the titration of inter- and intradomain carboxylate- and imidazole-containing side chains. The maximal increase in fluorescence, at pH ~4.5, was only slightly greater in the holotoxin than the isolated T domain, implying that the T domain accounts for most of the hydrophobic surface of DT accessible to TNS at low pH.

To study the low-pH-induced insertion of the T domain into membranes, we measured release of the fluorophore, ANTS, from SUVs that had been loaded with a mixture of ANTS and DPX (Mel & Stroud, 1993). DPX quenches the fluorescence of co-entrapped ANTS, resulting in low fluorescence of the intact SUVs. Release of ANTS and DPX into the surrounding buffer eliminates the quenching. T domain caused little release of ANTS at pH 5.25 or above, and the rate was half-maximal at pH 5.0. The rate of fluorophore release from vesicles in the first 10 s after

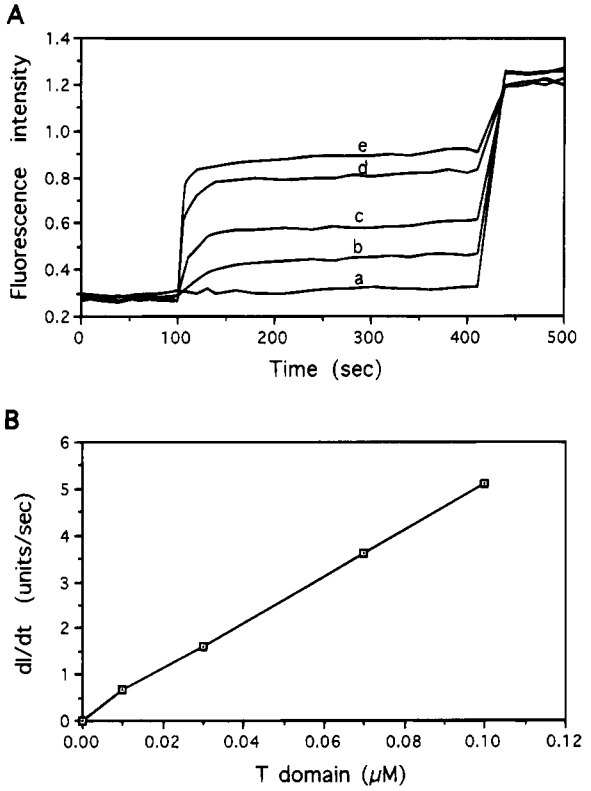

FIGURE 4: Release of ANTS and DPX from large unilamellar vesicles induced by T domain under acidic conditions. (A) Release at pH 5.0 as a function of T domain concentration. Different concentrations of T domain (a, control, no T domain; b, 10 nM; c, 30 nM; d, 70 nM; e, 100 nM) were mixed with vesicles at neutral pH. After 100 s the pH was lowered to 5.0. At 400 s detergent was added to lyse the vesicles to achieve complete release. (B) Initial rate of fluorophore leakage from liposomes as a function of T domain concentration. dI/dt, change of fluorescence intensity with time (dI/dt, arbitrary units) was derived from the results in panel A (first 10 s after lowering pH).

lowering the pH to 5.0 showed a linear dependence on T domain concentration over the range of 10−100 nM (Figure 4). Similar observations have been reported for certain pore forming toxins, including colicin E1 (Levinthal *et al.*, 1991) and colicin Ia (Mel & Stroud, 1993), suggesting that one molecule, or a single molecular complex, inserts into the membrane to form a channel.

To explore the potential of site-directed spin labeling in analyzing the T domain's interaction with membranes, we selected four residues (N235, S291, S332, and V351; Figure 1) for replacement by Cys and subsequent derivatization. S332 is located within hydrophobic helix TH8, which forms part of the buried hydrophobic hairpin (TH8−TH9). V351 is in the TL5 loop which forms the tip of the TH8−TH9 hairpin, and N235 and S291 are in loop regions of the other two helical layers of the domain (TL2 and TL3, respectively). All four mutant proteins retained reactivity with anti-DT polyclonal antibodies by western blot analysis, and they were stable for weeks at 4 °C in buffer containing 2 mM DTT.

Each protein was reacted with (1-oxyl-2,2,5,5-tetramethylpyrroline-3-methyl)methanethiosulfonate (I) to generate the nitroxide side-chain R1 (Figure 5). EPR spectra of the labeled mutants under various conditions are shown in Figure 6. All spectra reveal the presence of a small but variable amount of a "free" spin population (f), probably arising from nitroxide not attached to the protein. This amounts to no

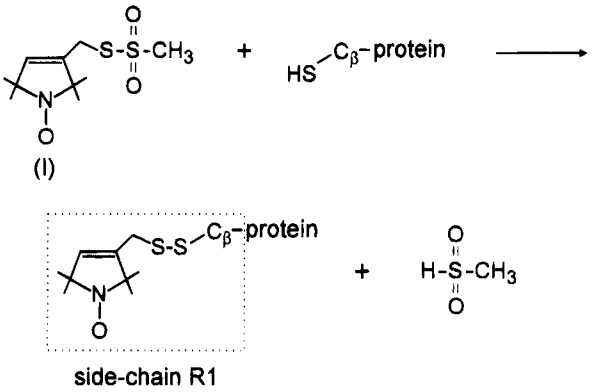

FIGURE 5: Reaction of the methanethiosulfonate spin label (I) with a cysteine residue to generate nitroxide side chain R1.

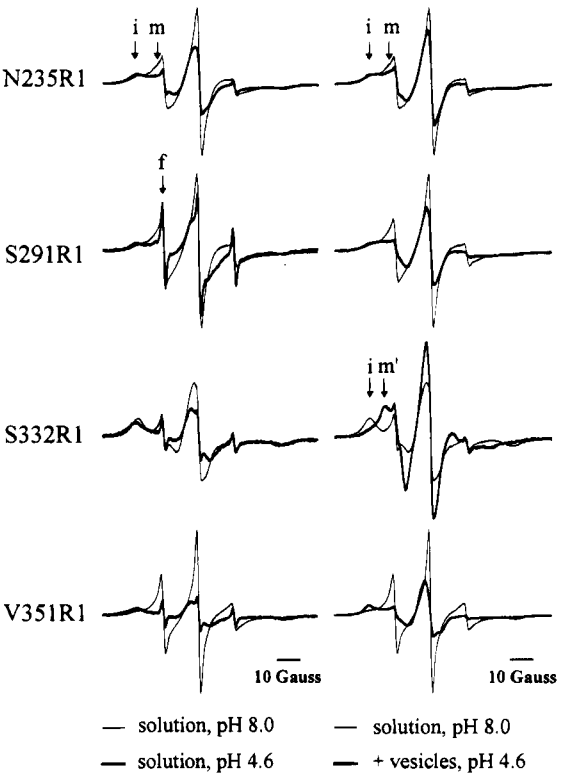

FIGURE 6: EPR spectra of T domain mutants. (Left-hand column) Spectra of T domain mutants in solution at pH 8.0 (light trace) and at pH 4.6 (heavy trace). (Right-hand column) Spectra of T domain mutants in solution at pH 8.0 (light trace) and in the presence of 17% POPG/POPC (mol/mol) vesicles at pH 4.6 (heavy trace). The spectra at pH 8.0 are the same in the presence and absence of vesicles. The spectra in each pair are normalized to represent the same number of spins. The arrows labeled i, m, and f identify components arising from immoblized, mobile, and "free" spin populations, respectively (see text). In the spectrum of S332R1 in the presence of membranes at pH 4.6, the arrow labeled m′ marks a resonance population with mobility intermediate between those of i and m.

more than a few percent of the total spin and will not be further considered. The line shapes of the mutants N235R1, S291R1, and V351R1 in aqueous solution at pH 8.0 (light traces) are complex and reflect at least two significant spin populations: one of high mobility (m) and the other more immobilized with respect to the protein (i). Since the protein contains only a single spin-labeled site, the populations must arise from different degrees of interaction of the nitroxide with the immediate environment in the protein.[2] The i state is attributed to nitroxides interacting with nearby structures

in the protein, while the m state arises from nitroxides projecting into solution, where the motion is limited primarily by rotational isomerization about the bonds which connect it to the backbone (Hubbell & Altenbach, 1994). This interpretation is consistent with the location of the nitroxides in N235R1, S291R1, and V351R1 predicted from the crystal structure of the T domain in DT (Choe *et al.*, 1992; Bennett *et al.*, 1994): in each of these mutants, the nitroxide is in a solvent-exposed interhelical loop, where it could make tertiary contacts with nearby helices (Figure 1). Alternatively, the i state could arise from quaternary interactions within an oligomer or aggregated state (see below).

The spectrum of S332R1 in solution consists essentially of a single component with a line shape characteristic of a nitroxide immobilized with respect to the protein, indicating strong tertiary interactions of the side chain. Again, this is in accord with the solution structure of DT, in which Ser-332 is located within the hydrophobic core of the T domain.

The topographical location of an R1 side chain in a protein can be evaluated by examination of the collison frequencies of the nitroxide with nonpolar and polar paramagnetic reagents in solution (Hubbell & Altenbach, 1994a,b). Molecular O_2 is the choice for the nonpolar reagent, while the electrically neutral complexes NiAA and NiEDDA are suitable polar reagents. The collision rate of a nitroxide with these reagents is characterized by the proportional "accessibility parameter" Π, derived from the power saturation behavior of the nitroxide in the presence of the reagents (Farahbakhsh *et al.*, 1992). Nitroxide side chains buried in the protein interior have very low collison rates with any of the reagents, due to low solubility and diffusion coefficients in the protein interior (Altenbach *et al.*, 1990). On the other hand, solvent-exposed surface sites have relatively high collision rates with the polar NiAA and NiEDDA. For a membrane-bound protein, a nitroxide exposed to the fluid hydrophobic interior of the bilayer has a high collision rate with O_2 but a low rate with NiAA or NiEDDA. This contrast results from solubility differences of the reagents in the bilayer interior.

Values of $\Pi(O_2)$ and Π(NiEDDA) for the T domain mutants in solution are shown in Figure 7 panels a and c, respectively. A distinctive feature is the low accessibility of the nitroxide in S332R1 to either reagent. This is consistent with the immobilized line shape (Figure 6) and the buried location of S332 in the crystal structure. The accessibility to O_2 is higher than that for NiEDDA, presumably due to its smaller size and low polarity. The accessibilities of nitroxides at the other sites are high for both reagents, as expected from their surface locations. This conclusion applies to the m state of the nitroxide at these sites, because the experimental protocol for estimating accessibility heavily weights the more mobile compenent in multicomponent spectra.

When a solution containing the spin-labeled T domain at pH 8.0 was acidified to pH 4.6, significant changes in the EPR spectra took place at some sites (Figure 6, left-hand column). For nitroxides in the interhelical loops (N235R1, S291R1, and V351R1), acidification resulted in large increases in the i population at the expense of the m population. This could be due to oligimerization involving the surface of the T domain defined by these labeled sites (Figure 1). However, in none of the samples was macroscopic aggregation noted: the samples remained clear, and centrifugation at 15000*g* for 5 min yielded no loss of EPR signal in the supernatant and no detectable sediment. The EPR spectrum of the buried site S332R1 showed a slight change corresponding to an increase in the rotational correlation time.

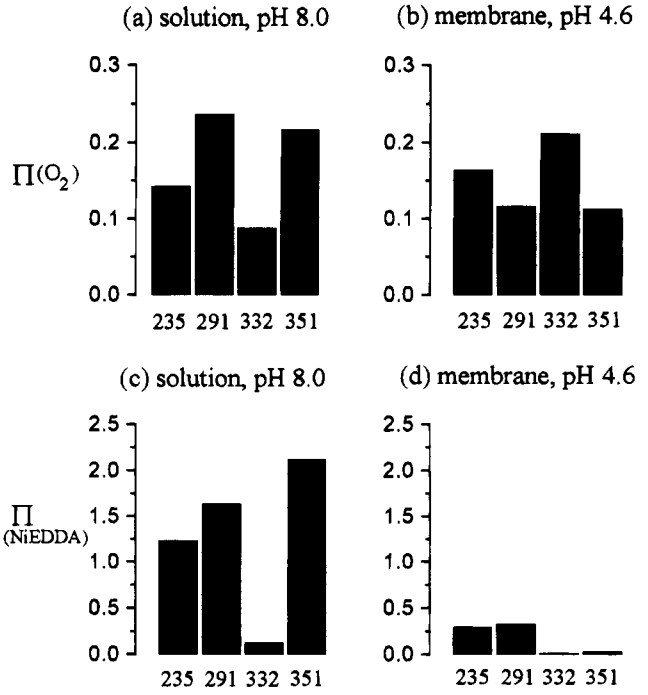

FIGURE 7: Accessibility parameters of the nitroxide spin labels. Accessibility parameters of oxygen ($\Pi(O_2)$) and NiEDDA (Π(NiEDDA)) for the spin labels at the indicated residues were measured in solution at pH 8.0 (a and c) and in the presence of 17% POPG/POPC (mol/mol) vesicles (b and d) as described in Materials and Methods. The concentration of O_2 was that in equilibrium with air, and the concentration of NiEDDA was 20 mM. The low concentration of NiEDDA chosen permitted differentiation of the accessibilities of the various side chains of the protein in solution.

When the spin-labeled T domain samples were mixed with 17% POPG/POPC vesicles at pH 8.0, no EPR spectral changes were noted (Figure 6, right-hand column, light trace). However, when the pH was shifted to 4.6, spectral changes similar, but not identical, to those noted above were observed for N235R1, S291R1, and V35R1 (Figure 6, right-hand column, heavy trace). The T domain was clearly associated with the vesicles as evidenced by the fact that the EPR signal remained with the vesicle pellet formed by centrifugation at 15000*g* for 5 min. Further evidence for an association is provided by the large spectral changes observed for S332R1, where the i population is nearly completely converted to a more mobile state (m′), indicating a decrease in tertiary interaction at this site. At the same time, the accessibilities to O_2 increases, whereas that with NiEDDA remains low (Figure 7). These changes are unambiguously interpreted as a movement of the nitroxide in S332R1 from a buried site within the protein to a lipid-exposed surface site as the protein binds to the membrane.

[2] The methanethiosulfonate spin label used in these studies has a high selectivity for cysteine and does not undergo detectable reaction with other amino acids under the conditions employed (Altenbach *et al.*, 1989). Thus all major components detected in the spectra arise from a single labeled site.

Size exclusion chromatography of the T domain (S291R1) in solution at pH 8 revealed a predominantly monomeric species with an elution time corresponding to a molecular weight of approximately 24 000 (actual MW = 19 184). However, smaller amounts of species corresponding to the dimer and larger aggregates were also present. The presence of these oligomeric forms could account for the i component in the solution spectra of N235R1, S291R1, and V351R1 at pH 8.0, as noted above. At pH 4.6, the T domain eluted at the void volume of the column (MW ≥ 100 000). This acid-induced oligomerization can readily account for the increase in the population of the i state in the spin-labeled derivatives when the pH is shifted from 8.0 to 4.6 (Figure 6). However, acidification of the T domain in the presence of vesicles apparently leads to association of the protein with the membrane, rather than to self-association in solution, as illustrated by the spectral changes that occur at S332R1 (Figure 6, right-hand column). We assume this also to be the case for the other labeled mutants.

Altenbach et al. (1994) have shown that the parameter $\phi(O_2,NiAA) = \ln\{\Pi(O_2)/\Pi(NiAA)\}$ varies linearly with depth in the membrane for a series of R1 side chains on the outer surface of a bacteriorhodopsin transmembrane helix. A similar relationship applies for $\phi(O_2,NiEDDA)$, and, in the presence of 200 mM NiEDDA and O_2 in equilibrium with air, the functional relationship is $\phi(O_2,NiEDDA) = 0.3d - 3$, where d is the penetration depth in angstroms measured from the plane of the phosphate groups of the phospholipids (C. Altenbach, D. Greenhalgh, H. G. Khorana, and W. L. Hubbell, unpublished).[3] In the present experiments, NiEDDA was used instead of NiAA, because of the poor stability of the latter complex at low pH. Under these conditions, $\phi(O_2,NiEDDA)$ for the nitroxide in membrane-bound S332R1 is 1.5, corresponding to $d = 15$ Å. Thus residue 332 is near the center of the bilayer. Given the central location of S332 on a hydrophobic face of TH8, this finding is consistent with the proposal that the TH8−TH9 helical hairpin inserts into and spans the bilayer in the membrane-bound state (Choe *et al.,* 1992). However, these data alone cannot distinguish this model from one in which the TH8 helix lies parallel to the membrane surface, since the sum of the helix diameter and side chain length is roughly 15 Å. Depth determinations with other spin-labeled mutants along the length of this helix could resolve this matter.

For N235R1, S291R1, and V351R1, a striking decrease in accessibility of the nitroxide to NiEDDA was observed upon acidification in the presence of the vesicles (Figure 7). This is in accord with the decrease in mobility at these sites (Figure 6). Whatever the structure of the membrane-bound protein, it is difficult to reconcile the strong immobilization and sequestration of the nitroxide at V351R1 with a simple helical hairpin inserted across the bilayer. The increase in O_2 accessibility at N235R1 is indicative of an intramembrane location for this site. However, the depth of penetration cannot be reliably estimated due to the immobilization of the nitroxide that could result in different steric effects for O_2 and NiEDDA and invalidate the analysis based on the ϕ function (Altenbach *et al.,* 1994).

[3] The concentration of NiEDDA for this experiment is an order of magnitude higher than that used to obtain the data in Figure 7 because of the low partitioning of NiEDDA into the membrane interior.

The results presented show that the isolated T domain of DT retains, to a first approximation, the basic functional properties ascribed to it from studies with whole DT. It is soluble and largely monomeric at neutrality or slightly basic pH and inserts into and permeabilizes bilayers when the pH is reduced to pH ~5. Elsewhere we have shown that the T domain forms ion-conductive channels in planar bilayers, which are essentially indistinguishable from those formed by the holotoxin (Mindell *et al.*, 1994). These characteristics are consistent with earlier observations that the B45 fragment (residues 194−386 from CRM45, a chain termination protein of diphtheria toxin; Giannini *et al.,* 1984) is water-soluble at neutral pH and forms channels in planar bilayers under acidic conditions (Kagan *et al.,* 1981). Spin labels attached at four separate sites gave data basically consistent with the solution structure of the toxin at pH 8.0 and with insertion of the T domain under acidic conditions. On the basis of these results, one can proceed to a more extensive application of site-directed spin labeling and work toward a detailed model of the structure of the integral membrane form of the T domain. Such information may yield insights into the mechanism by which the T domain facilitates passage of the toxin's catalytic domain across the endosomal membrane.

ACKNOWLEDGMENT

We thank M. J. Bennett and D. Eisenberg for sharing the refined DT crystal structure prior to publication, S. Choe for discussion in early phases of the work, J. Milne and P. Hanna for critical reading of the manuscript, and C. Altenbach for preparation of Figure 1.

REFERENCES

Altenbach, C., Flitsch, S. L., Khorana, H. G., & Hubbell, W. L. (1989) *Biochemistry 28*, 7806−7812.

Altenbach, C., Marti, T., Khorana, H. G., & Hubbell, W. L. (1990) *Science 248*, 1088−1092.

Altenbach, C., Greenhalgh, D. A., Khorana, H. G., & Hubbell, W. L. (1994) *Proc. Natl. Acad. Sci. U.S.A. 91*, 1667−1671.

Ausubel, F., Brent R., Kingston, R., Moore, D., Seidman, J., Smith, J., & Struhl, K., Eds. (1987) *Current Protocols in Molecular Biology*, Greene-Wiley Interscience, New York.

Bennett, M. J., & Eisenberg, D. (1994) *Protein Sci. 3,* 1464−1475.

Bennett, M. J., Choe, S., & Eisenberg, D. (1994) *Protein Sci. 3,* 1444−1463.

Böttcher, C. J. F., Van Gent, C. M., & Pries, C. (1961) *Anal. Chim. Acta. 24*, 203−204.

Choe, S., Bennett, M. J., Fujii, G., Curmi, P. M. G., Kantardjieff, K. A., Collier, R. J., & Eisenberg, D. (1992) *Nature 357*, 216−222.

Collier R. J. (1990) in *ADP-Ribosylating Toxins and G Proteins: Insights into Signal Transduction* (Moss J., & Vaughan M., Eds.) pp 3−19, American Society for Microbiology, Washington, D.C.

Dumont, M. E., & Richards, F. M. (1988) *J. Biol. Chem. 263*, 2087−2097.

Farahbakhsh, Z. T., Altenbach, C., & Hubbell, W. L. (1992) *Photochemistry and Photobiology 56*, 1019−1033.

Giannini, G., Rappuoli, R., & Ratti, G. (1984) *Nucleic Acids Res. 12*, 4063−4069.

Greenfield, L., Bjorn, M. J., Horn, G., Fong, D., Buck, G. A., Collier, R. J., & Kaplan, D. A. (1983) *Proc. Natl. Acad. Sci. U.S.A. 80*, 6853−6857.

Hovde, C. J., Calderwood, S. B., Mekalanos, J. J., & Collier, R. J. (1988) *Proc. Natl. Acad. Sci. U.S.A. 85*, 2568−2572.

Hubbell, W. L., & Altenbach, C. (1994a) in *Membrane Protein Structure: Experimental Approaches* (White, S., Ed.) pp 224−248, Oxford University Press, London.

Hubbell, W. L., & Altenbach, C. (1994b) *Curr. Opin. Struct. Biol. 4*, 566−573.

Hubbell, W. L., Froncisz, W., & Hyde, J. S. (1987) *Rev. Sci. Instrum. 58*, 1879−1886.
Kagan, B. L., Finkelstein, A., & Colombini, M. (1981) *Proc. Natl. Acad. Sci. U.S.A. 78*, 4950−4954.
Koehler, T., & Collier, R. J. (1991) *Mol. Microbiol. 5*, 1501−1506.
Kraulis, P. J. (1991) *J. Appl. Crystallogr. 24*, 946−950.
Levinthal, F., Todd, A. P., Hubbell, W. L., & Levinthal, C. (1991) *Proteins: Struct., Funct., Genet. 11*, 254−262.
London, E. (1992) *Mol. Microbiol. 6*, 3277−3282.
McClare, C. W. (1971) *Anal. Biochem. 39*, 527−530.
Mel, S. F., & Stroud, R. M. (1993) *Biochemistry 32*, 2082−2089.
Mindell, J. A., Zhan, H., Huynh, P. D., Collier, R. J., & Finkelstein, A. (1994) *Proc. Natl. Acad. Sci. U.S.A. 91*, 5272−5276.
Naglich, J. G., Metherall, J. E., Russell, D. W., & Eidels, L. (1992) *Cell 69*, 1051−1061.
O'Keefe, D. O. (1992) *Arch. Biochem. Biophys. 269*, 678−684.
O'Keefe, D. O., Cabiaux, V., Choe, S., Eisenberg, D., & Collier, R. J. (1992) *Proc. Natl. Acad. Sci. U.S.A. 89*, 6202−6206.
Olsnes, S., Kozlov, J. V., van Deurs, B., & Sandvig, K. (1991) *Semin. Cell Biol. 2*, 7−14.
Sandvig, K., & Olsnes, S. (1981) *J. Biol. Chem. 256*, 9068−9076.
Shin, Y. K., Levinthal, C., Levinthal, F., & Hubbell,W. L. (1993) *Science 259*, 960−963.
Silverman, J. A., Mindell, J. A., Finkelstein, A., Shen, W. H., & Collier, R. J. (1994) *J. Biol. Chem. 269*, 22542−22532.
Studier, F. W., & Moffatt, B. A. (1986) *J. Mol. Biol. 189*, 113−130.
Szoka, F., & Papahadjopoulos, D. (1978) *Proc. Natl. Acad. Sci. U.S.A. 75*, 4194−4198.

BI942906L